HISTOMORPHOLOGY OF THE HYPOBRANCHIAL GLAND IN *DICATHAIS ORBITA* (GMELIN, 1791) (NEOGASTROPODA: MURICIDAE)

C. B. WESTLEY[1]*, M. C. LEWIS[2] AND K. BENKENDORFF[1]

[1]*School of Biological Sciences, Flinders University, GPO Box 2100, Adelaide, SA 5001, Australia; and*
[2]*Department of Anatomy and Histology, Flinders University, GPO Box 2100, Adelaide, SA 5001, Australia*

**Correspondence: C.B. Westley; e-mail: chantel.westley@flinders.edu.au*

(Received 22 June 2009; accepted 30 November 2009)

ABSTRACT

Tyrian purple is a dye used in antiquity and is a natural product of marine molluscs of the family Muricidae. Bioactive precursors of Tyrian purple occur in the hypobranchial gland, reproductive glands and egg masses of muricids, such as *Dicathais orbita*. Histomorphological examination of the hypobranchial–gonoduct complex (rectum and hypobranchial, capsule, albumen and rectal glands) was conducted to provide the first description of the hypobranchial gland in *D. orbita* and to determine a mechanism for the transfer of Tyrian purple precursors to the gonoduct and ultimately to the egg masses. Seven secretory cell types were identified in the hypobranchial epithelium of *D. orbita*, which can be broadly classified into cells containing mucoproteins and acidic sulphated mucopolysaccharides. Three secretory cells new to the Muricidae were identified, along with two cell types that appear to be associated with synthesis of Tyrian purple. A subepithelial vascular sinus surrounding the rectum and rectal gland occurs between the hypobranchial gland and gonoduct. Examination of this region failed to reveal a direct anatomical mechanism for the transfer of precursors to the gonoduct. However, biochemical similarities in secretions from the hypobranchial, capsule and albumen glands suggest that the synthesis of precursors within the gonoduct may be possible.

INTRODUCTION

Tyrian purple is a natural dye that has been used in several cultures since antiquity. It is synthesized in the hypobranchial gland of muricid gastropods from the prochromogen, tyrindoxyl sulphate (Baker & Sutherland, 1968). By action of an arylsulphatase enzyme, cytotoxic and antimicrobial intermediates are generated (Benkendorff, Bremner & Davis, 2000; Westley, Vine & Benkendorff, 2006; Vine *et al*., 2007) and in the presence of sunlight, the intermediate tyriverdin is photolytically cleaved to produce Tyrian purple (Cooksey, 2001). The production of Tyrian purple also occurs in muricid egg masses (Palma, Paredes & Cristi, 1991; Benkendorff *et al*., 2000; Benkendorff, Bremner & Davis, 2001; Benkendorff, Westley & Gallardo, 2004), which has prompted investigation into a possible reproductive role for the bioactive intermediates (Westley *et al*., 2006; Westley & Benkendorff, 2008a).

Egg capsule formation in the Muricidae is facilitated by a suite of specialized glandular structures. The albumen gland secretes perivitelline fluid around the eggs before they are passed to the capsule gland for encapsulation and eventually to the ventral pedal gland for the deposition of outer capsule laminae (Westley & Benkendorff, 2008b) and attachment to the substrate (Fretter, 1941). Observations of purple pigmentation in capsule glands of *Dicathais orbita* (Gmelin, 1791) and *Concholepas concholepas* (Bruguière, 1789) (Benkendorff *et al*., 2004) imply that bioactive intermediates may be incorporated into egg masses as a form of maternal investment in larval chemical defence (Westley *et al*., 2006). A maternal source for Tyrian purple precursors in muricid egg masses has recently been supported by detection of the prochromogen in albumen gland extracts and, additionally, of bioactive intermediates in the capsule gland of *D. orbita* (Westley & Benkendorff, 2008a). The capsule gland presents a likely site for incorporation of both precursors and biosynthetic enzymes from the adjacent hypobranchial gland during capsule formation (Westley & Benkendorff, 2008a). Similarly, the albumen gland may facilitate prochromogen inclusion into albuminous secretions (Westley & Benkendorff, 2008a). The ventral pedal glands are also of potential interest, because precursors may be incorporated during deposition of the outer capsule lamina. Overall, the presence of hypobranchial gland metabolites in muricid egg masses and the female gonoduct suggests that precursors are either transferred from their site of synthesis in the maternal hypobranchial gland or synthesized within reproductive glands.

Histomorphological attributes of the gonoduct (Fretter, 1941; Ramorino, 1975; Kool, 1988; Jaramillo, 1991; Middelfart, 1992a, b; Aungtonya, 1997; Westley, 2008) and hypobranchial gland (Bernard, 1890; Letellier, 1890; Erspamer, 1946; Bolognani-Fantin & Ottaviani, 1981; Srilakshmi, 1991; Roller, Rickett & Stickle, 1995; Naegel & Aguilar-Cruz, 2006) have been reported for many Muricidae. However, previous investigations have dealt with the gonoduct and hypobranchial gland separately, so that an anatomical mechanism for precursor transfer between these structures may have been overlooked. Similarly, the potential for precursor synthesis within the gonoduct has not been considered. Correlations between the histochemistry of the gonoduct and capsule laminae have recently been employed to establish the process of encapsulation in the Pulmonata (Pal, 2007) and Muricidae (Westley & Benkendorff, 2008b). Similarly, correlations between gonoduct and hypobranchial gland biochemistry may provide preliminary evidence for the production of synonymous gonoduct and hypobranchial gland secretions. Consequently, we aim to present the first detailed description

of hypobranchial gland in *D. orbita* and, in addition, to address the histomorphology of the hypobranchial–gonoduct complex to establish a mechanism for the incorporation of precursors of Tyrian purple in muricid egg masses.

MATERIAL AND METHODS

Twelve female specimens of *Dicathais orbita* were sampled from subtidal rocky platforms along the Fleurieu Peninsula of South Australia during 2005–2006. Sex was determined by the presence of albumen, ingesting and capsule glands and the absence of a penis. The shell length of each live specimen was measured from spire to siphonal canal (to 0.01 mm) with vernier callipers. The average size of specimens was 54.94 $\pm$ 12.36 cm. The shell was then removed by cracking with a vice at the junction of the body whorl and spire, and the soft body removed by severing the columellar muscle. The soft body was then transferred to a dissecting tray and submersed in filtered (0.22 μm) seawater to reduce osmotic stress. The dorsal mantle and pallial gonoduct were separated from the rest of the visceral mass by an incision along the lateral margins of the columellar muscle. For gross morphological descriptions, digital images of the dorsal mantle were taken with a stereo-dissecting microscope (Olympus, SZH). The mantle was then folded back and pinned with the ventral surface facing up. Images of the hypobranchial gland epithelium and capsule, ingesting and albumen glands and seminal receptacles were then acquired.

Longitudinal and transverse incisions were made along the junction between the ctenidium and branchial–hypobranchial epithelium, and the ingesting gland and digestive gland, respectively. The hypobranchial–gonoduct complex, including the pallial gonoduct complete with dorsal mantle, rectum, and rectal and hypobranchial glands, was then fixed in 10% neutral buffered formalin for 6 h, dehydrated through an ethanol series, cleared in chloroform and embedded in paraffin. At least 18 serial transverse sections (5 μm) were obtained from five regions of interest for all 12 specimens. These regions included the anterior pallial gonoduct, medial capsule gland, posterior capsule gland, anterior ingesting gland and the posterior ingesting gland, which also contains the albumen gland and seminal receptacles. Six replicate sections from each region were stained with: (1) Modified Harris Haematoxylin and Eosin Y with Phloxine B (Thompson, 1966) or Lillie–Mayer's Haematoxylin and Eosin (Lillie, 1977) for routine histological description (abbreviation: HE); (2) Periodic Acid Schiff (McManus, 1946) for the demonstration of mucous cells; and (3) Toluidine Blue (Kramer & Windrum, 1954) for the differentiation of neutral (Wägele, Ballesteros & Avila, 2006), sulphated (Kramer & Windrum, 1954) and phenol-acid mucopolysaccharides (Ramalingam & Ravindranath, 1970). Sections were examined under a compound light microscope (Olympus, BH-2) and measurements of hypobranchial gland cells were obtained with an eyepiece micrometer (to 0.01 μm) from epithelial regions prominent for each cell type. Cell type classification was determined for mature cells only; these were epithelial cells with a full complement of secretory products that were observed to be exocytosed. Cells possessing identical secretory morphology and biochemistry, consistent cell morphology and comparable distribution across 12 adult females were classified as a specific cell type.

RESULTS

Gross morphology of the hypobranchial–gonoduct complex

The ventral surface of the dorsal mantle of *Dicathais orbita* is characterized by an anteroposteriorly elongated hypobranchial gland, which extends from the left lateral ctenidium (Fig. 1A) to surround the ventral surface of the rectum, capsule and ingesting gland on the right (Fig. 1B). The rectum is embedded in the left lateral portion of the pallial gonoduct,

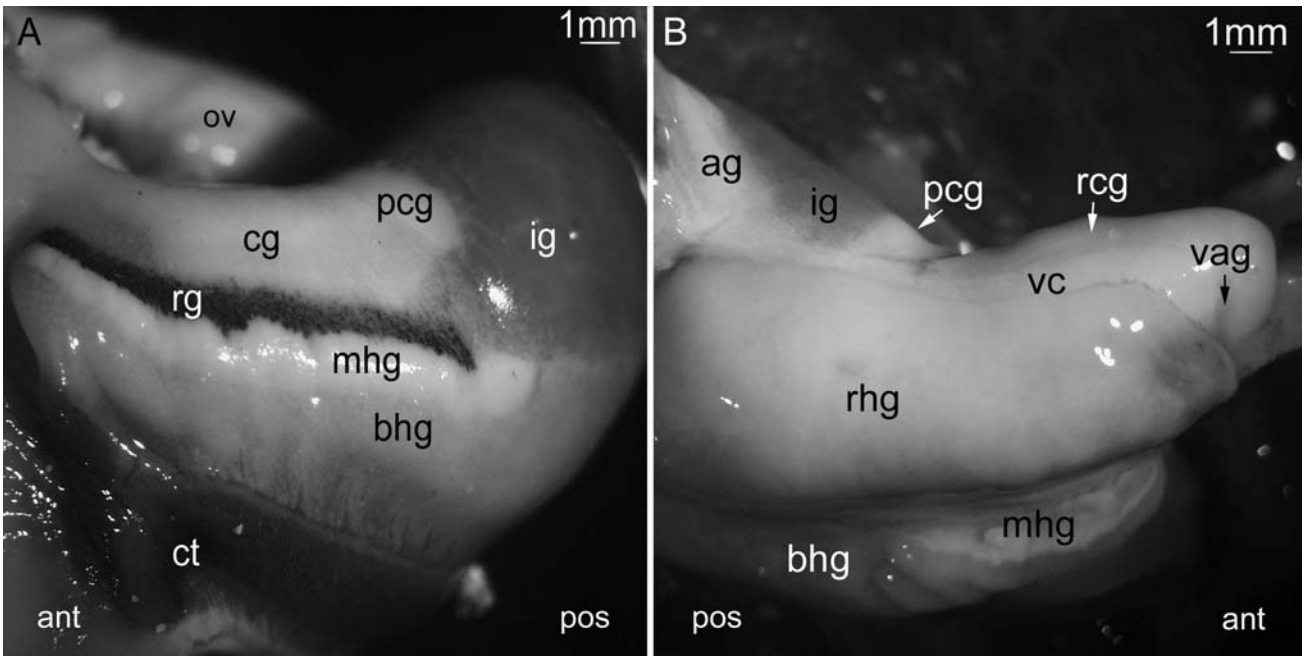

Figure 1. The gross morphology of the hypobranchial–gonoduct complex of a female *Dicathais orbita*. **A.** Anterodorsal view from the left of the pallial gonoduct and hypobranchial gland. **B.** Anteroventral view from the right side. Abbreviations: ag, albumen gland; ant, anterior; cg, capsule gland; ct, ctenidium; bhg, branchial hypobranchial region; mhg, medial hypobranchial region; rhg, rectal hypobranchial region; ig, ingesting gland; ov, ovary; pcg, posterior capsule gland lobe; pos, posterior; rcg, right capsule gland lobe; rg, rectal gland; vag, vaginal opening; vc, ventral channel. Scale bars = 1 mm.

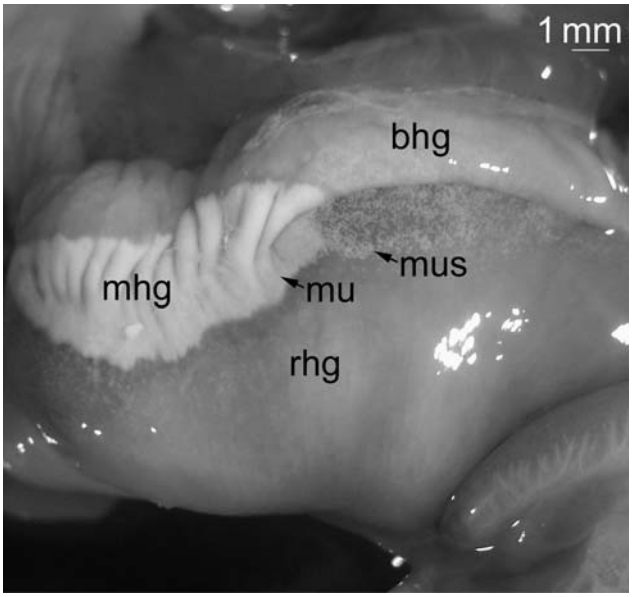

Figure 2. Mucus on the ventral surface of the hypobranchial gland in *Dicathais orbita*. Abbreviations: bhg, branchial hypobranchial region; mhg, medial hypobranchial region; mu, mucus; mus, mucus spherules; rhg, rectal hypobranchial region. Scale bar = 1 mm.

which occupies the right side of the mantle cavity. From anterior to posterior, the gonoduct is comprised of capsule, ingesting and albumen glands (Fig. 1A, B). The capsule gland is a white glandular mass composed of two lateral lobes, a dorsal and a posterior lobe (Fig. 1B). A prominent rectal gland lies dorsal to the capsule gland (Fig. 1A). A laterally compressed, sigmoid-shaped albumen gland is partially embedded in the posterioventral portion of the ingesting gland on its right side (Fig. 1B).

The hypobranchial gland is divided into three well-defined sections, a left branchial region, an adjacent medial region and a right rectal region (Fig. 2). The lateral regions extend from the vaginal opening to the albumen gland (Fig. 1B) and the epithelium is composed of transverse folds, orientated perpendicular to the mantle. The medial region exists as a slight depression between the branchial and rectal regions (Fig. 1B), and can be seen, through the dorsal integument, to commence and terminate with the capsule and rectal gland (Fig. 1A). The medial region was invariably covered in a viscous, cream-coloured secretion (Fig. 2), which appeared successively yellow, red, green and purple after exposure to oxygen and light, and produced a pungent sulphurous odour indicative of the pigmented indoxyl sulphate precursors of Tyrian purple. Minute secretory spherules were observed on the proximal rectal and branchial epithelium, while distal regions appeared to be devoid of secretion (Fig. 2).

Pallial gonoduct histomorphology

The vaginal opening leads to the ventral channel, which is a semi-enclosed duct developed from left and right longitudinal folds (Fig. 3A). The ventral channel maintains this morphology posteriorly, ventral to the right capsule gland lobe (Fig. 1B). Upon reaching the anterior ingesting gland, the folds unite with the ventral musculature creating a closed duct. The ventral channel then opens into the dorsal albumen gland at the posterior of the ingesting gland.

The anterior capsule gland is composed of four distinct lobes: an anteroventral lobe, a small dorsal lobe, and left and right lateral lobes (Fig. 3A). A dorsoventral lumen lined with ciliated columnar epithelium is formed between the lateral lobes (Fig. 3A) and receives secretion from all four lobes. The anteroventral lobe divides the ventral portion of the dorsoventral lumen into transverse lumina, with the left one opening into the ventral channel (Fig. 3A). Acini of the anteroventral lobe contain a spherical secretion, which stains lightly eosinophilic, orthochromatically with Toluidine Blue and is positive for Periodic Acid Schiff (PAS) (Fig. 3A). Identical acini also make up the ventral portion of the right lateral lobe (Fig. 3A). The lateral lobes are also acinous in arrangement and the secretion is similarly packaged in spherules, but these stain strongly eosinophilic, and lightly orthochromatic with

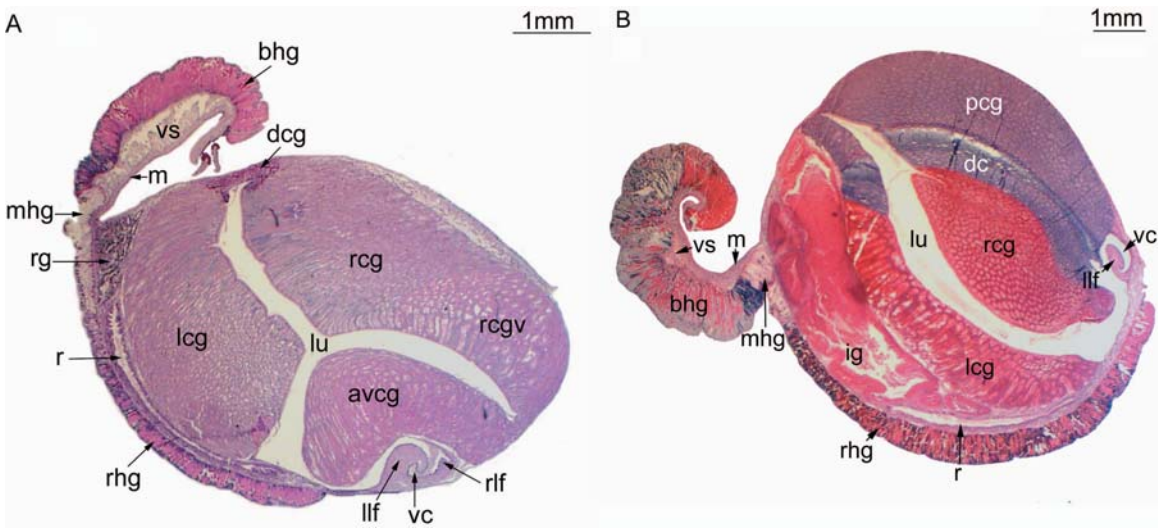

Figure 3. Transverse sections through the anterior gonoduct of a female *Dicathais orbita* showing the lobed configuration of the capsule gland and the relative positioning of the hypobranchial gland and associated structures. **A.** The anterior capsule gland stained with PAS. **B.** The posterior capsule gland stained with HE. Abbreviations: avcg, anteroventral capsule gland lobe; bhg, branchial hypobranchial region; dc, dorsal lobe cells; dcg, dorsal capsule gland lobe; ig, ingesting gland; lcg, left capsule gland lobe; llf, left longitudinal fold; lu, lumen; m, mantle; mhg, medial hypobranchial region; pcg, posterior capsule gland lobe; r, rectum; rcg, right capsule gland lobe; rcgv, ventral portion of right capsule gland lobe; rg, rectal gland; rhg, rectal hypobranchial region; rlf, right longitudinal fold; vc, ventral channel; vs, vascular sinus. Scale bars = 1 mm.

Toluidine Blue and PAS (Fig. 3A). The dorsal lobe is composed of comparatively large subepithelial secretory cells, loosely arranged into acini. These cells release an amorphous basophilic and weakly PAS-positive secretion (Fig. 3A), which stains metachromatically purple with Toluidine Blue.

The posterior capsule gland is divided into a right posterior lobe lined anteroventrally with dorsal lobe cells, and remnant right and left lobes (Fig. 3B). Just anterior to the posterior lobe, the anteroventral lobe fuses with the right lobe. Posteriorly, the left and right lobes are replaced by the anterior ingesting gland and posterior lobe, respectively. This arrangement opens the ventral channel directly into the dorsoventral lumen (Fig. 3B). The acinous posterior lobe secretes basophilic (Fig. 3B), PAS-positive spherules into the ventral channel, which also stain metachromatic purple with Toluidine Blue.

The albumen gland is composed of left and right lobes joined by a thin suture (Fig. 4). As occurs in the capsule gland, subepithelial acini release secretory products into a dorsoventral lumen lined with a ciliated columnar epithelium. Two secretory products arise from the albumen gland. The more plentiful amorphous secretion is eosinophilic, stains orthochromatically with Toluidine Blue and is PAS-positive (Fig. 4), while the second is basophilic and stains metachromatic purple with Toluidine Blue. Seminal receptacles line the dorsal and posterior periphery of the albumen gland (Fig. 4) and open into the lumen of the dorsal albumen gland. The ciliated, cuboidal epithelium lining the receptacles is devoid of secretion and subepithelial acini are absent.

Two ventral pedal glands are present in female *D. orbita*. The anterior pedal gland appears as a specialized region of mantle epithelium, ventral to the medial capsule gland. The epithelium is composed of ciliated pseudostratified columnar cells interspaced with goblet cells. The secretion of columnar cells is eosinophilic (Fig. 5A) and stains orthochromatically with Toluidine Blue. The posterior ventral pedal gland emerges from the ventral mantle of the ingesting gland as a prominent muscular papilla (Fig. 4). Anteriorly, the ciliated columnar epithelium is simple and comprised of eosinophilic and basophilic secretory cells (Fig. 5B) interspaced with goblet cells. Posteriorly, the epithelium is pseudostratified and arranged into longitudinal folds with more numerous goblet cells (Fig. 5C) and isolated basophilic secretory cells. The eosinophilic secretion stains orthochromatically with Toluidine Blue and is PAS-positive, while the basophilic secretion fails to stain with PAS or Toluidine Blue. The posterior ventral pedal gland was also observed to receive secretions from the rectal hypobranchial gland epithelium in two individuals (Fig. 5D).

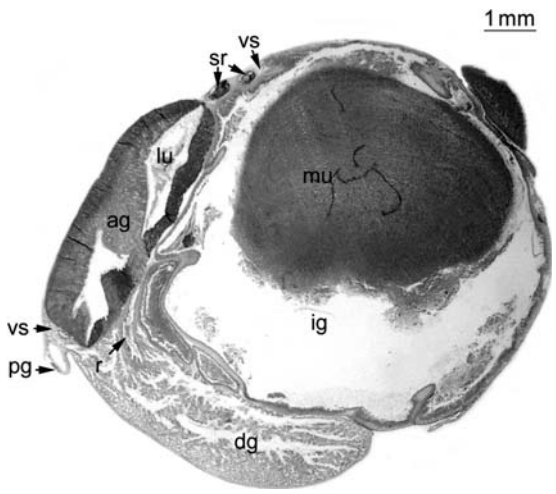

Figure 4. A transverse section through the posterior gonoduct of a female *Dicathais orbita* stained with PAS. Abbreviations: ag, albumen gland; dg, digestive gland; ig, ingesting gland; lu, lumen; mu, mucus; pg, posterior ventral pedal gland; r, rectum; sr, seminal receptacles; vs, vascular sinus. Scale bar = 1 mm.

Hypobranchial gland histomorphology

The hypobranchial gland is composed of tall ciliated and nonciliated pseudostratified columnar epithelial cells (Fig. 6A–D). Based on location of cell types, the branchial and rectal regions can be further subdivided into proximal and distal portions. All regions of the hypobranchial gland are separated from the adjacent gonoduct, rectum and rectal gland by a continuous sinus composed of vascular spaces supported by loose connective tissue (Figs 3A, 5A). The basal lamina rests on a thin layer of subepithelial smooth muscle, which extends a short distance between the glandular folds. At least seven different secretory cell types, along with additional ciliated supportive cells, characterize the hypobranchial epithelium of *D. orbita* (Table 1).

Ciliated supportive cells represent the most common cell type, and are located between secretory cells (Fig. 6A–D) throughout all three regions of the hypobranchial gland. These cells possess the morphology of a funnel, which rapidly tapers from the epithelial surface towards the basal lamina. Although the course of these cells can be traced a considerable way into the epithelium, their slender form, coupled with the distended nature of adjacent secretory cells, renders it difficult to confirm a connection with the basal lamina. The apical nucleus is spindle shaped (Fig. 6B) and the eosinophilic cytoplasm (Fig. 6D) stains orthochromatically with Toluidine Blue (Fig. 6C).

Type I secretory cells (Fig. 6A–D) are cylindrical in shape, possess round basal nuclei, prominent nucleoli and are extremely wide (Table 1). These cells dominate the distal portion of rectal (Fig. 6A) and branchial regions, where they alternate with various combinations of other secretory cells. These cells are less numerous proximally (Fig. 6B, C), although isolated cells still remain in the medial region (Fig. 6D). The secretion contains large eosinophilic spherules (Table 1), which appear partly to coalesce in distal lateral cells, but gain separate integrity moving towards the medial region. Toluidine Blue staining intensity from weak to strong (Table 1) correlates with secretion morphology from distal to proximal cells, respectively. Spherules are golden in unstained sections.

Elongate basophilic granules are characteristic of secretory cell type II (Fig. 6A). These cells appear to alternate with cell type I in the distal lateral regions (Fig. 6A) and are also a prominent feature of the proximal portions, but are absent from the medial epithelium (Fig. 6D). These cells are comparatively slender, devoid of apical cilia (Table 1) and possess round basal nuclei and nucleoli. The secretion is packaged into elongate granules, which appear to maintain this morphology until exocytosed into the mantle cavity. Basophilic granules exhibit weak metachromasia with Toluidine blue (Table 1). Cell type III is commonly paired with type II and, likewise, shares a similar distribution (Fig. 6A). Although the morphology of these cells is almost identical, the biochemistry of their secretions differs (Table 1). When tightly packed, the apices stain orthochromatically with Toluidine Blue, while loosely packed granules exhibit green metachromasia (Table 1). In the absence of Phloxine B, granules stained eosinophilic (Table 1) while, in its presence, granules appeared brownish-green.

Cells reminiscent of goblet cells typify type IV secretory cells (Table 1). These cells possess elongate basal nuclei, distinct nucleoli and are commonly scattered throughout the proximal lateral regions (Fig. 6B), while isolated cells may

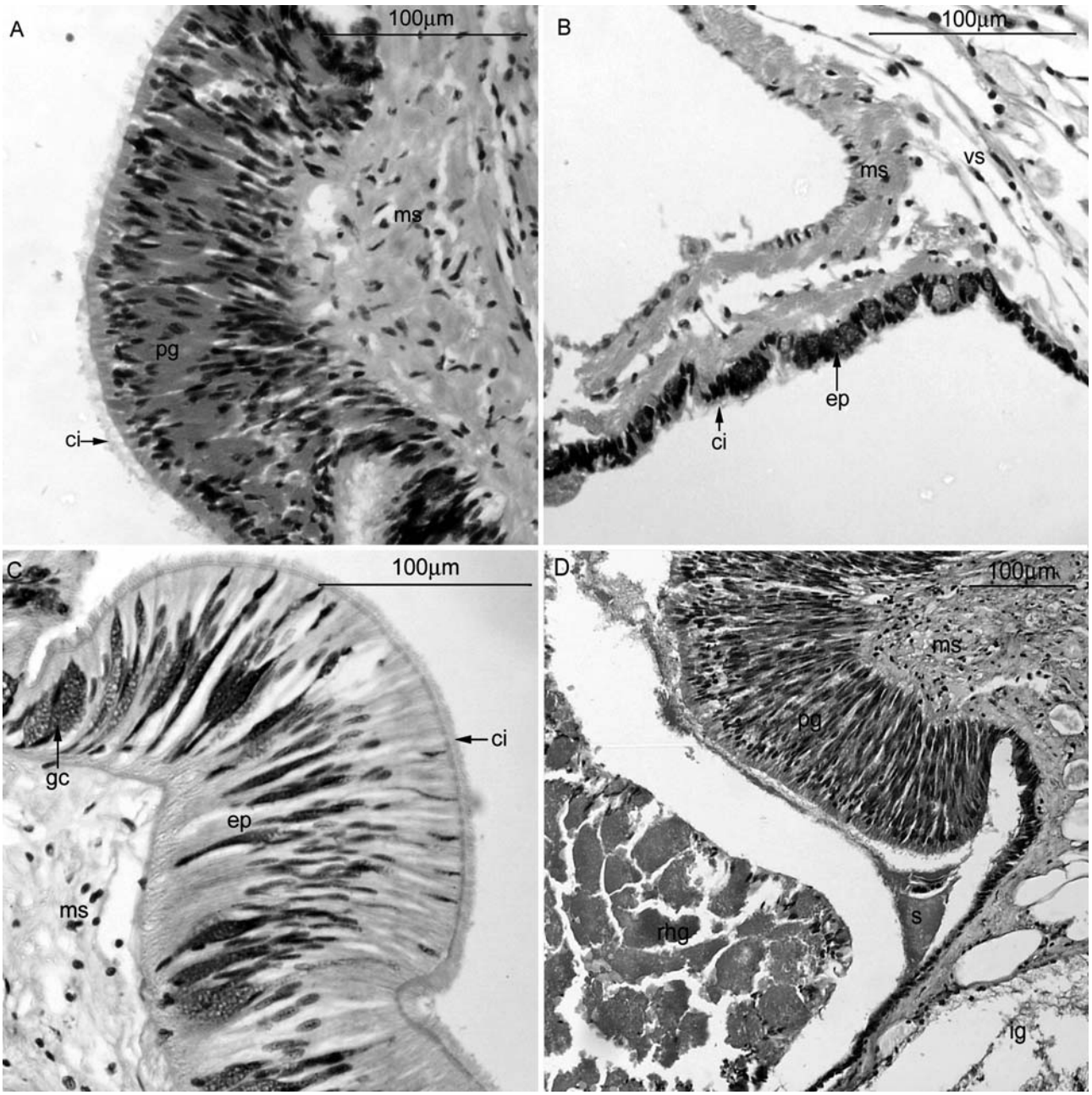

Figure 5. The ventral pedal glands of a female *Dicathais orbita*. **A.** The anterior ventral pedal gland stained with HE. **B.** The simple anterior epithelium of the posterior ventral pedal gland stained with HE. **C.** The folded posterior epithelium of the posterior ventral pedal gland stained with PAS. **D.** The posterior ventral pedal gland receiving secretions from the rectal hypobranchial gland stained with HE. Abbreviations: ci, cilia; gc, goblet cell; ep, epithelium; ig, ingesting gland; ms, muscle; pg, pedal gland; rhg, rectal hypobranchial region; s, secretions; vs, vascular sinus. Scale bars = 100 µm.

also be present in the distal portion. Secretory spherules appear to remain membrane-bound until released from the cell. Type V secretory cells (Fig. 5B) contain an unusual basophilic exudate with a thread-like morphology (Table 1). Cylindrical, with a dense round nucleus, this cell type appears, partly, to replace secretory cell type I in the proximal portion of the branchial and rectal regions of some individuals. The medial region of the hypobranchial epithelium is dominated by secretory cell type VI (Fig. 6D), although isolated cells may also occur in the lateral regions (Fig. 6A, B). These cells are cylindrical in morphology, comparatively large (Table 1) and possess dense elongate nuclei. Initial observation showed these cells to be empty, as the cytoplasm failed to stain with any of the methods applied (Table 1). However, on close examination, large secretory spherules can be seen, faintly outlined by background staining. Secretory cell type VII is also comparatively large (Fig. 5C) with a round basal nucleus and nucleolus. These cells are characterized by an amorphous secretion, which stains strongly metachromatic purple with Toluidine Blue (Table 1). Cells of this type are characteristic of the proximal branchial region (Fig. 6C), although they may extend distally in the anterior epithelium. Isolated cells were also observed in the rectal region of some individuals.

Secretory cell distribution varied considerably among individuals. However, paired cell types II and III were commonly

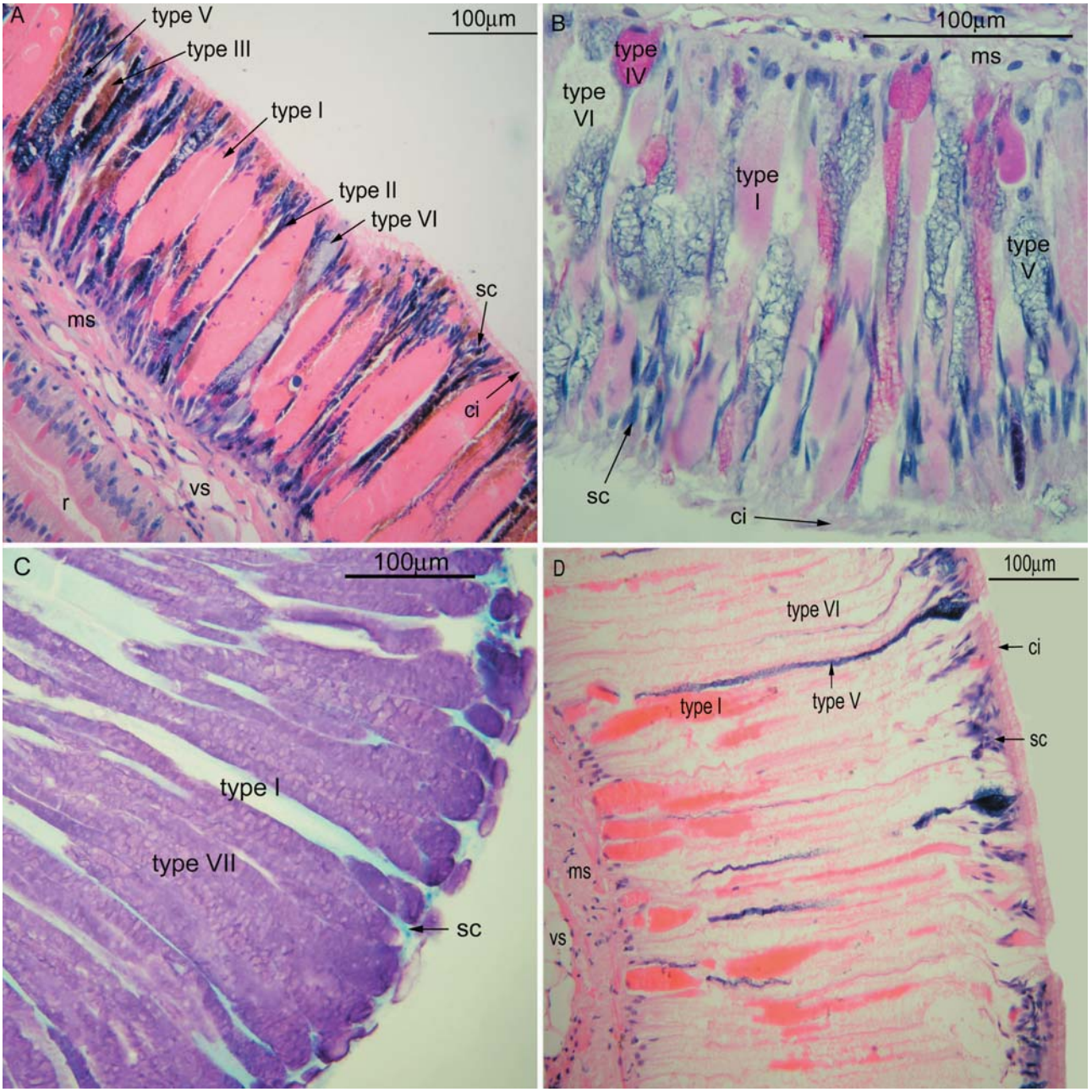

Figure 6. Transverse sections showing the seven types of secretory cells (Types I–VII) and supportive cells (sc) characteristic of the hypobranchial epithelium of *Dicathais orbita*. **A.** The distal rectal epithelium stained with HE. **B.** The proximal rectal epithelium stained with PAS. **C.** The proximal branchial epithelium stained with Toluidine Blue. **D.** The medial epithelium stained with HE. Abbreviations: ci, cilia; ms, muscle; r, rectum; vs, vascular sinus. Scale bars = 100 µm.

observed to extend from the proximal into the distal portion of both lateral regions. In such individuals, these slender cells alternated with cell type V rather than type I cells. Anteriorly, secretory cells with basophilic amorphous secretion (type VII) appeared to dominate the branchial epithelium and, in some cases, this dominance was maintained posteriorly.

Rectal gland and rectum histomorphology

The rectal gland is visible through the dorsal mantle as a dark, pigmented, anteroposteriorly elongated structure, adjacent to the medial hypobranchial gland (Fig. 1A). The anterior rectal gland appears to open into the mantle cavity, while the posterior terminates with the medial hypobranchial gland at the posterior capsule gland (Fig. 1A). The rectal gland is acinous in arrangement, with up to 30 acini composed of ciliated cuboidal epithelial cells with dense apical nuclei and isolated goblet cells (Fig. 7). The subepithelium is devoid of gland cells or musculature, but is rich in vascular spaces supported by loose connective tissue (Fig. 7). Dark green-brown pigments (0.65 ± 0.07 µm) occupy the cytoplasm of each epithelial cell (Fig. 7). Despite their prevalence in the epithelium, these pigments are absent from the longitudinal lumina (Fig. 7).

The rectum commences anteriorly as a longitudinally folded duct, surrounded by a thin layer of circular muscle, which opens into the mantle cavity via the anus. The rectum is positioned ventral to the rectal gland, left and dorsal to the

Table 1. The morphological and histochemical properties of secretory cells composing the hypobranchial epithelium of *Dicathais orbita*.

Type	Cilia	Dimensions ± SD (μm)		Secretion	Haem	Eosin	PAS	Toluidine Blue	
		Height	Width					Ortho	Meta
Sup	Yes	*	*	Homo	−	+	−	+	−
I	No	306.17 ± 65.21	34.27 ± 9.78	Spherules	−	++	+	+/++	−
II	No	255.55 ± 79.56	4.3 ± 1.09	Granules	++	−	−	−	Purple (+)
III	No	255.38 ± 80.66	4.3 ± 0.88	Granules	−	++	−	+	Green (+)
IV	No	183.74 ± 13.23	*	Spherules	−	++	++	+	−
V	No	194.53 ± 33.19	18.82 ± 4.41	Thread-like	+	−	−	−	−
VI	No	201.87 ± 11.87	15.97 ± 2.86	Spherules	−	−	−	−	−
VII	No	503.72 ± 37.27	21.24 ± 4.45	Amorphous	+	−	+	−	Purple (++)

Abbreviations: haem, haematoxylin; homo, homogeneous; meta, metachromatic; ortho, orthochromatic; sup, supportive cell; −, negative; +, weakly positive; ++, strongly positive. $n = 4$ specimens, $n = 5$ cells of each type/specimen.

*Mean dimensions were unable to be determined due to constriction by adjacent cells.

vaginal opening, and is enveloped on its ventral surface by the rectal hypobranchial gland (Fig. 3A, B). Posteriorly, the rectum elongates dorsoventrally in unison with the left capsule gland lobe and the rectal hypobranchial gland (Fig. 3A). The rectum maintains this morphology until the anterior ingesting gland, where the lumen shortens ventrally (Fig. 3B) and terminates once again as a longitudinally folded duct, ventral to the ingesting gland (Fig. 4).

Ciliated pseudostratified columnar epithelial cells line the lumen, which is invariably occupied by waste material. Goblet cells interspaced with secretory cells containing two types of cytoplasmic spherules characterize the rectum epithelium. One type is weakly eosinophilic (Fig. 6A) and stains orthochromatically with Toluidine Blue, while the second is strongly eosinophilic (Fig. 6A) and PAS-positive. In unstained sections, these latter spherules appear golden. Waste material within the lumen stains in an identical manner to the former secretion (Fig. 6A), although minute endogenous brown pigments may also be present.

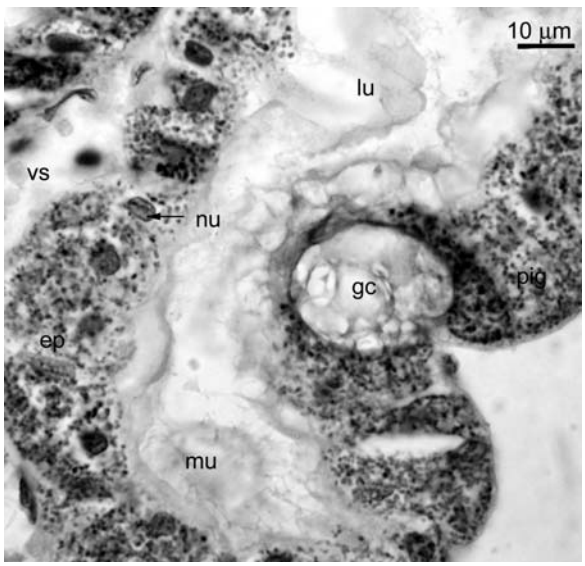

Figure 7. A transverse section through the rectal gland of *Dicathais orbita* stained with PAS. Abbreviations: ep, epithelium; gc, goblet cells; lu, lumen; mu, mucus; nu, nucleus; pig, endogenous pigments; vs, vascular sinus. Scale bar = 10 μm.

DISCUSSION

Histomorphological examination of the hypobranchial–gonoduct complex was conducted to provide the first description of the hypobranchial gland in *Dicathais orbita* and to discover a mechanism for the inclusion of Tyrian purple precursors in muricid egg masses. The hypobranchial gland of *D. orbita* is divided into branchial, medial and rectal regions (Figs 2, 3A, B). Nerve cells were not observed in the hypobranchial gland of *D. orbita*, despite proposed neurological control over secretion release in *Nucella lapillus* (Bernard, 1890), *Buccinum undatum* (Hunt, 1973) and *Morula granulata* (Srilakshimi, 1991). In *D. orbita*, secretions appear to be released through subepithelial muscular stimuli, as suggested for *Stramonita canaliculata* (Roller *et al*., 1995).

The hypobranchial epithelium of *D. orbita* is characterized by ciliated supportive cells and at least seven secretory cell types (Table 1). Ciliated supportive cells arise between groups of secretory cells (Fig. 6A–D) and are thought to provide support through the formation of intracellular junctions (Hunt, 1973). Similar cells also occur in *B. undatum* (Hunt, 1973), *Murex brandaris* (Bolognani-Fantin & Ottoviani, 1981), *Morula granulata* (Srilakshmi, 1991), *S. canaliculata canaliculata* (Roller *et al*., 1995) and various opisthobranchs (Wägele *et al*., 2006). Although these cells play no apparent role in the secretion process, they may assist in combining secretory products released from adjacent cells and moving secretion over the epithelial surface (Hunt, 1973).

All secretions from the hypobranchial gland of *D. orbita* remain membrane-bound until exocytosed from the cell where they are directed to the medial depression. In contrast, secretions from the posterior distal rectal region appear to be driven towards the posterior ventral pedal gland (Fig. 5D). This may facilitate the transfer of hypobranchial secretions to the outer lamina of egg capsules during capsule molding. However, as the outer lamina degrades within 1 week of deposition (Lim *et al*., 2007), secretions from the pedal gland fail to explain the high concentration of Tyrian purple precursors present in capsules during the remainder of the encapsulation period (Benkendorff *et al*., 2000). Thus, an alternative mode of incorporating bioactive intermediates into egg capsules for embryonic chemical defence remains to be identified in the Muricidae.

Two secretory cell types appear to occur exclusively within muricid hypobranchial glands, which suggest they may be associated with Tyrian purple synthesis. Cell type I contains large eosinophilic spherules (Fig. 6A) that stain for proteins and carbohydrates (Table 1). Spherules were observed to coalesce in

distal cells, but gain separate integrity towards the medial region. Cells displaying a similar shift in secretion morphology have also been reported in the muricid *Plicopurpura pansa* (Naegel & Aguilar-Cruz, 2006). Secretory cell type VI is characteristic of the medial hypobranchial epithelium of *D. orbita* (Fig. 6D) and is characterized by large secretory spherules that failed to stain with any of the methods applied (Table 1). These cells may correspond to the 'empty' or 'clear' cells reported in all muricids studied to date (Bolognani-Fantin & Ottaviani, 1981; Srilakshmi, 1991; Roller *et al*., 1995; Naegel & Aguilar-Cruz, 2006). The absence of these cells from non-muricid species (Tarao, 1935; Ronkin, 1952; Hunt, 1973; Ottaviani, 1978) supports a role in Tyrian purple production. Early investigations of *N. lapillus* (Letellier, 1890; Bernard, 1890) identified cells of the medial zone as 'purple-producing'. Later, Erspamer (1946) demonstrated the presence of prochromogen in the posterior and anterior medial hypobranchial gland of *Hexaplex trunculus* and *M. brandaris*, respectively, while arylsulphatase was limited to the anterior medial region in both species. Thus, it is possible that unstained spherules contain tyrindoxyl sulphate or arylsulphatase. Intracellular localization of these compounds is required to resolve the composition of secretions and confirm the contribution of cell types I and VI to the synthesis of Tyrian purple.

As type I and VI secretory cells appear to be associated with Tyrian purple synthesis in *D. orbita*, sites for precursor transfer to adjacent albumen and capsule glands, where precursors have been detected (Westley & Benkendorff, 2008a), may be associated with these cells. The hypobranchial gland is separated from the capsule gland by a subepithelial vascular sinus (Fig. 3A) and terminates just anterior to the albumen gland (Fig. 4). No direct connection in the form of a duct was observed between any region of the hypobranchial epithelium and the capsule or albumen glands. Furthermore, examination of the basal lamina failed to provide evidence for the release of secretory products into subepithelial vascular spaces. Nevertheless, the vascular sinus is continuous between the hypobranchial, capsule (Fig. 3A, B) and albumen (Fig. 4) glands and may provide a means of transferring hypobranchial metabolites to the gonoduct and ultimately to the egg masses. Alternatively, bioactive precursors may be synthesized from endogenous prochromogen in the gonoduct. Evolutionary trends in the organisation of gastropod mantle cavity organs from an ancestral bilateral arrangement to a loss of all posttorsional right organs suggest that the gonoduct of caenogastropods has developed from an ancestral right hypobranchial gland (Fretter *et al*., 1998). Consequently, the capacity for the synthesis of precursors of Tyrian purple may have been retained in the reproductive glands of some Muricidae over the course of evolution. This would theoretically facilitate both the synthesis of hypobranchial gland metabolites in the pallial gonoduct and their inclusion in muricid egg masses.

Similarities between the secretory products of hypobranchial gland cells thought to be involved in Tyrian purple synthesis and those of various gonoduct secretions are evident in this investigation. The staining reactions of spherules within hypobranchial gland cell type I (Table 1) correlate with those of the anteroventral and lateral capsule gland lobes and the perivitelline secretion from the albumen gland. Furthermore, the highly sulphated secretion of hypobranchial gland cell type VII (Table 1) is reminiscent of secretions from the dorsal and posterior capsule gland lobes and the less plentiful albumen gland secretion. As tyrindoxyl sulphate is a sulphate ester of indoxyl (Cooksey, 2001), it is possible that sulphur is sourced from mucopolysaccharides in both hypobranchial gland cell type VII and the pallial gonoduct.

Although a direct mode for the transfer of precursors of Tyrian purple was not confirmed, examination of structures associated with the hypobranchial gland may shed light on the origin of primary metabolites for Tyrian purple synthesis. Dietary-derived tryptophan is the most likely origin of the Tyrian purple prochromogen (Westley *et al*., 2006). The rectum occupies the subepithelial vascular sinus to the right of the rectal hypobranchial gland and ventral to the rectal gland (Fig. 3A, B). Endocytosed eosinophilic spherules in rectal epithelial cells possess golden endogenous pigmentation and stain for mucoproteins. These show remarkable similarity to spherules of type I hypobranchial secretory cells, which suggest that tryptophan may be acquired from waste in the rectum for prochromogen synthesis in the hypobranchial gland. The rectal gland also shares this vascular sinus (Fig. 3A, B) in *D. orbita* and other Muricidae (Kool, 1993; Roller *et al*., 1995; Naegel & Aguilar-Cruz, 2006). This gland functions in the catabolism of haemolymph macromolecules such as tyrosine, which is evidenced by the deposition of melanin in epithelial cells (Andrews, 1992). It is possible that degradation of the tryptophan-containing respiratory pigment, haemocyanin (Waxman, 1975; Avissar, Daniel and Daniel, 1986), also occurs in rectal epithelial cells. The intimate association between the rectal gland and the medial hypobranchial epithelium (Fig. 1A), where dye secretions accumulate, warrants further investigation into the immediate distribution of this amino acid.

Of the secretory cells identified, three new cell types in addition to those previously reported for gastropod hypobranchial glands were observed. Cell type II secretes weakly acidic sulphated mucopolysaccharides, type III contains elongate eosinophilic granules composed of neutral and phenol-acid mucopolysaccharides, while the biochemical properties of type V remain unclear (Table 1). In contrast, goblet cells rich in glycoprotein (type IV) have been reported in neogastropods of the Muricidae (Bolognani-Fantin & Ottaviani, 1981; Srilakshmi, 1991; Roller *et al*., 1995; Naegel & Aguilar-Cruz, 2006), Buccinidae (Hunt, 1973) and Melongenidae (Ronkin, 1952), basal caenogastropods of the Viviparidae (Ottaviani, 1978) and vetigastropods of the Haliotidae (Tarao, 1935). The wide distribution of these cells throughout Gastropoda reaffirms the primary function of this gland in the production of mucus to facilitate the binding and removal of particulate matter introduced in the respiratory current (Fretter & Graham, 1994).

Hypobranchial secretory cells containing highly sulphated mucopolysaccharides (type VII) also appear common to the Neogastropoda (Ronkin, 1952; Hunt, 1973; Srilakshmi, 1991) and shelled opisthobranchs (Wägele *et al*., 2006). Dermatan/chondroitin sulphate, heparin and heparan sulphate are common sulphated mucopolysaccharide components, which are ubiquitous in vertebrates and invertebrates (Nader *et al*., 1999). These biological response modifiers are involved in fibrogenesis (Trowbridge & Gallo, 2002), antimicrobial defence and coagulation, and cell–cell recognition (Nader *et al*., 1999), respectively. All three have been isolated from mantle tissue of the bivalve *Anomalocardia brasiliana* (Nader *et al*., 1984, 1999), while the latter two (Nader *et al*., 1984) and compounds of comparable molecular structure and activity occur in other molluscs (Burson *et al*., 1956; Pancake & Karnovsky, 1971; Cassaro & Dietrich, 1977), including the caenogastropod *Pomacea* (Nader *et al*., 1984). In addition to the removal of particulate matter, it has been suggested that the hypobranchial gland may assist in the binding and eradication of potential pathogens (Westley *et al*., 2006). Although structural elucidation of these sulphated mucopolysaccharides is required, coagulation, cell recognition and microbial defence

within hypobranchial gland secretions would complement such a role.

Overall, histomorphological comparison of the hypobranchial epithelium in *D. orbita* with other Muricidae, lower caenogastropod and vetigastropod species has revealed two cell types which appear specific to Tyrian purple synthesis. Although a direct anatomical means for precursor transfer between the hypobranchial gland and gonoduct was not detected in *D. orbita*, the subepithelial vascular sinus adjoining glands of the hypobranchial–gonoduct complex may provide a potential transport mechanism. Alternatively, similarities in hypobranchial and gonoduct secretion biochemistry suggest the precursors may be synthesized in the capsule or albumen glands. Novel histochemical techniques for the detection of compounds and biosynthetic enzymes required for Tyrian purple genesis have recently been developed (Westley, 2008) to allow further investigation into this proposed source of intermediates in muricid egg masses.

ACKNOWLEDGEMENTS

We would like to thank, S.P. Kool, R. Jaramillo, P. Middelfart and W.F. Ponder for their assistance during early anatomical examinations. We greatly appreciate the provision of a Flinders University Postgraduate Scholarship to C. Westley. This research was supported by a Philanthropic research grant to K. Benkendorff.

REFERENCES

ANDREWS, E.B. 1992. The fine structure and function of the anal gland of the muricid, *Nucella lapillus* (Neogastropoda) (and a comparison with that of the trochid *Gibbula cineraria*). *Journal of Molluscan Studies*, **58**: 297–313.

AUNGTONYA, C. 1997. Structure of the capsule gland of *Chicoreus capucinus* (Lamarck, 1822) and *Chicoreus ramosus* (Linnaeus, 1758). *Phuket Marine Biological Center Special Publication*, **17**: 89–92.

AVISSAR, I., DANIEL, E. & DANIEL, V. 1986. Haemocyanin mRNA from arthropod and mollusc origin. *Biochemical Journal*, **233**:253–257.

BAKER, J. & SUTHERLAND, M. 1968. Pigments of marine animals VIII. Precursors of 6,6′-dibromoindigotin (Tyrian purple) from the mollusc *Dicathais orbita* (Gmelin). *Tetrahedron Letters*, **1**: 43–46.

BENKENDORFF, K., BREMNER, J.B. & DAVIS, A.R. 2000. Tyrian purple precursors in the egg masses of the Australian muricid, *Dicathais orbita*: a possible defense role. *Journal of Chemical Ecology*, **26**: 1037–1050.

BENKENDORFF, K., BREMNER, J.B. & DAVIS, A.D. 2001. Indole derivatives from the egg masses of muricid molluscs. *Molecules*, **6**: 70–78.

BENKENDORFF, K., WESTLEY, C.B. & GALLARDO, C.S. 2004. Observations on the production of purple pigments in the egg capsules, hypobranchial and reproductive glands from seven species of Muricidae. *Invertebrate Reproduction and Development*, **46**: 93–102.

BERNARD, F. 1890. Glande à mucus. Secretion du mucus. Chapter 1: Histologie de glande à mucus. In: Recherches sur les organs palleaux. *Annales des Sciences Naturelles Zoologie*, **9**: 296–305.

BOLOGNANI-FANTIN, A.M. & OTTAVIANI, E. 1981. The hypobranchial gland of some Prosobranchia (Mollusca: Gastropoda) living in different habitats: a comparative histochemical study. *Monitore Zoologico Italiano*, **15**: 63–76.

BURSON, S.L., FAHRENBACH, M.J., FROMMHAGEN, L.H., RICCARDI, B.A., BROWN, R.A., BROCKMAN, H.V., LEWRY, H.V. & STOKSTAD, E.L.R. 1956. Isolation and purification of mactins, heparin-like anticoagulants from the Mollusca. *Journal of the American Chemical Society*, **78**: 5874–5878.

CASSARO, C.M.F. & DIETRICH, C.P. 1977. The distribution of sulphated mucopolysaccharides in invertebrates. *Journal of Biological Chemistry*, **252**: 2254–2261.

COOKSEY, C.J. 2001. Tyrian Purple: 6,6′-dibromoindigo and related compounds. *Molecules*, **6**: 736–769.

ERSPAMER, V. 1946. Ricerche chimiche e farmacolgiche sugli estratti di ghiandola ipobranchiale di *Murex* (*Truncularia*) *trunculus* (L.), *Murex* (Biolinus) *brandaris* (L.) e *Tritonalia erinacei* (L.). *Pubblicazioni della Stazione Zoologica di Napoli*, **20**: 91–101.

FRETTER, V. 1941. The genital ducts of some British stenoglossan prosobranchs. *Journal of the Marine Biological Association of the United Kingdom*, **25**: 173–211.

FRETTER, V. & GRAHAM, A. 1994. *British prosobranch molluscs: their functional anatomy and ecology*. Ray Society, London.

FRETTER, V., GRAHAM, A., PONDER, W.F. & LINDBERG, D.R. 1998. Prosobranchs: introduction. In: *Mollusca: the southern synthesis. Fauna of Australia*. Vol. 5, Part B (P.L. Beesley, G.J.B. Ross & A. Wells eds), pp. 605–638. CSIRO Publishing, Melbourne.

HUNT, S. 1973. Fine structure of the secretory epithelium in the hypobranchial gland of the prosobranch gastropod *Buccinum undatum* L. *Journal of the Marine Biological Association of the United Kingdom*, **53**: 59–71.

JARAMILLO, R. 1991. Female genital system of *Chorus giganteus* (Prosobranchia: Muricidae). *Veliger*, **34**: 297–301.

KOOL, S.P. 1988. Aspects of the anatomy of *Plicopurpura patula* (Prosobranchia: Muricidae: Thaidinae), new combination, with emphasis on the reproductive system. *Malacologica*, **29**: 373–382.

KOOL, S.P. 1993. Phylogenetic analysis of the Rapaninae (Neogastropoda: Muricidae). *Malacologia* **35**: 155–259.

KRAMER, H. & WINDRUM, G.M. 1954. The metachromatic staining reaction. *Journal of Histochemistry and Cytochemistry*, **3**: 227–237.

LETELLIER, A. 1890. Recherches sur la poupre produite par le *Purpura lapillus*. *Archives de Zoologie Experimentale et Génerale*, **8**: 361–407.

LILLIE, R.D. 1977. *H. J. Conn's Biological Stains*. Edn 9. Williams and Wilkins Co., Baltimore.

LIM, N.S.H., EVERUSS, K.J., GOODMAN, A.E. & BENKENDORFF, K. 2007. Comparison of surface microfouling and bacterial attachment on the egg capsules of two molluscan species, representing the Cephalopoda and Neogastropoda. *Aquatic Microbial Ecology*, **47**: 275–287.

McMANUS, J.F.A. 1946. Histological demonstration of mucin after periodic acid. *Nature*, **158**: 202.

MIDDELFART, P. 1992a. Morphology and anatomy of *Chicoreus brunneus* (Link, 1807): description of shell and soft part. *Phuket Marine Biological Center Special Publication*, **11**: 54–60.

MIDDELFART, P. 1992b. Morphology and anatomy of *Chicoreus ramosus* (Linnaeus, 1758) soft parts. *Phuket Marine Biological Center Special Publication*, **11**: 66–71.

NADER, H.B., CHAVANTE, S.F., DOS-SANTOS, E.A., OLIVEIRA, T.W., DE-PAIVA, J.F., JERÔNIMO, S.M., MEDEIROS, G.F., DE-ABREU, L.R., LEITE, E.L., DE-SOUSA-FILHO, J.F., CASTRO, R.A., TOMA, L., TERSARIOL, I.L., PROCIONATTO, M.A. & DIETRICH, C.P. 1999. Heparan sulphates and heparins: similar compounds performing the same functions in vertebrates and invertebrates? *Brazilian Journal of Medical and Biological Research*, **32**: 529–538.

NADER, H.B., FERREIRA, T.M.P.C., PAVIA, J.F., MEDEIROS, M.G.L., JERÔNIMO, S.M.B., PAVIA, V.M.P. & DIETRICH, C.P. 1984. Isolation and structural studies of heparan sulfates and chondroitin sulphates from three species of molluscs. *Journal of Biological Chemistry*, **259**: 1431–1435.

NAEGEL, L. & AGUILAR-CRUZ, C.A. 2006. The hypobranchial gland from the purple snail *Plicopurpura pansa* (Gould, 1853) (Prosobranchia: Muricidae). *Journal of Shellfish Research*, **25**: 391–394.

OTTAVIANI, E. 1978. A gland system of the hypobranchial type in the mantle of *Paludina vivipara* draparnaud (Gastropoda: Prosobranchia): a morphological and histochemical study. *Monitore Zoologico Italiano*, **12**: 77–86.

PAL, P. 2007. Fine structure of reproductive glands in two primitive marine pulmonates (Basommatophora: Siphonariidae). *Acta Zoologica*, **88**: 145–152.

PALMA, H., PAREDES, J.C. & CRISTI, E. 1991. 6,6′-Dibromoindigotin en capsulas de embriones de *Concholepas concholepas* (Bruguiere 1789). *Medio Ambiente*, **11**: 93–95.

PANCAKE, S.J. & KARNOVSKY, M.L. 1971. The isolation and characterization of a mucopolysaccharide secreted by the snail, *Otella lactea*. *Journal of Biological Chemistry*, **246**: 253–262.

RAMALINGAM, K. & RAVINDRANATH, M.H. 1970. Histochemical significance of green metachromasia to Toluidine blue. *Histochemistry and Cell Biology*, **24**: 322–327.

RAMORINO, L. 1975. Ciclo reproductivo de *Concholepas concholepas* en la zona de Valparaíso. *Revista de Biologia Marina Valparaíso*, **15**: 149–177.

ROLLER, R., RICKETT, J.D. & STICKLE, W.B. 1995. The hypobranchial gland of the estuarine snail *Stramonita haemastoma canaliculata* (Gray) (Prosobranchia: Muricidae): a light and electron microscopical study. *American Malacological Bulletin*, **11**: 177–190.

RONKIN, R.R. 1952. Cytological studies on mucus formation and secretion in *Busycon*. *Biological Bulletin*, **102**: 252–260.

SRILAKSHMI, G. 1991. The hypobranchial gland in *Morula granulata* (Gastropoda: Prosobranchia). *Journal of the Marine Biological Association of the United Kingdom*, **71**: 623–634.

TARAO, S. 1935. Microscopical study on the hypobranchial gland of *Haliotis japonica* Reeve with a note on the restitution of the secretion. *Zoology*, **4**: 103–117.

THOMPSON, S. 1966. *Selected histological and histopathological methods*. Thomas Books, Springfield, IL, USA.

TROWBRIDGE, J.M. & GALLO, R.L. 2002. Dermatan sulfate: new functions from an old glycosaminoglycan. *Glycobiology*, **12**: 117–125.

VINE, K.L., LOCKE, J.M., RANSOM, M., PYNE, S.G. & BREMNER, J.B. 2007. *In vitro* cytotoxicity evaluation of some substituted isatins. *Bioorganic and Medicinal Chemistry*, **15**: 931–938.

WÄGELE, H., BALLESTEROS, M. & AVILA, C. 2006. Defensive glandular structures in opisthobranch molluscs – from histology to ecology. *Oceanography and Marine Biology*, **44**: 197–276.

WAXMAN, L. 1975. The structure of arthropod and mollusc haemocyanins. *Journal of Biological Chemistry*, **250**: 3796–3806.

WESTLEY, C.B. 2008. The distribution, biosynthetic origin and functional significance of Tyrian purple precursors in the Australian muricid *Dicathais orbita* (Neogastropoda: Muricidae). PhD thesis, Flinders University, South Australia, pp. 43–85, 204–235.

WESTLEY, C.B. & BENKENDORFF, K. 2008a. Sex-specific Tyrian purple genesis: precursor and pigment distribution in the reproductive system of the marine mollusc, *Dicathais orbita*. *Journal of Chemical Ecology*, **34**: 44–56.

WESTLEY, C.B. & BENKENDORFF, K. 2008b. Histochemical correlations between egg capsule laminae and the female gonoduct reveal the process of capsule formation in the Muricidae (Neogastropoda: Mollusca). *Invertebrate Reproduction and Development*, **51**: 81–92.

WESTLEY, C.B., VINE, K. & BENKENDORFF, K. 2006. A proposed functional role for indole derivatives in reproduction and defense of the Muricidae (Neogastropoda: Mollusca). In: *Indirubin, the red shade of indigo* (L. Meijer, N. Guyard, A.L. Skaltsounis & G. Eisenbrand eds), pp. 31–44. Life in Progress Editions, Roscoff France.